Theor Chem Acc (2009) 123:237–247
DOI 10.1007/s00214-009-0519-y

REGULAR ARTICLE

Combinatorics of angular momentum recoupling theory: spin networks, their asymptotics and applications

Vincenzo Aquilanti · Ana Carla P. Bitencourt · Cristiane da S. Ferreira · Annalisa Marzuoli · Mirco Ragni

Received: 27 November 2008 / Accepted: 17 January 2009 / Published online: 11 February 2009

Abstract The quantum theory of angular momentum and the associated Racah–Wigner algebra of the Lie group $SU(2)$ have been widely used in many branches of theoretical and applied physics, chemical physics, and mathematical physics. This paper starts with an account of the basics of such a theory, which represents the most exhaustive framework in dealing with interacting many-angular momenta quantum systems. We then outline the essential features of this algebra, that can be encoded, for each fixed number $N = (n + 1)$ of angular momentum variables, into a combinatorial object, the *spin network graph*, where vertices are associated with finite-dimensional, binary coupled Hilbert spaces while edges correspond to either phase or Racah transforms (implemented by 6*j* symbols) acting on states in such a way that the quantum transition amplitude between any pair of vertices is provided by a suitable 3*nj* symbol. Applications of such a combinatorial setting—both in fully quantum and in semiclassical regimes—are briefly discussed providing evidence of a unifying background structure.

1 Introduction

The mathematical apparatus of quantum-mechanical angular momentum (re)coupling, developed originally to describe spectroscopic phenomena in atomic, molecular, optical, and nuclear physics, is embedded in modern algebraic settings which emphasize the underlying combinational structure. $SU(2)$ recoupling coefficients, or 3*nj* symbols, as well as the related problems of their calculations, general properties, asymptotic limits for large entries, play nowadays a prominent role also in quantum gravity and quantum computing applications. We refer to the ingredients of this theory—and possibly of its extension to other Lie and quantum groups—by using the collective term 'spin networks'.

Such a combinatorial setting, illustrated in Sect. 2, can be thought of as a sort of 'abacus' encoding diagrammatical rules encountered in quantum collision theory [30] or even as (families of) 'computational quantum graphs' able to process algorithmic problems arising in discrete mathematics and theoretical physics [55].

The basic angular momentum functions, namely the Clebsch–Gordan coefficient—or its symmetric counterpart given by the Wigner 3*j* symbol—and the Racah 6*j* symbol, can be easily associated with 'classical' hypergeometric polynomials in one discrete variable, denoted respectively by ${}_3F_2$ and ${}_4F_3$. Such functions were generalized in terms of *q*-analogs [35, 51, 60] and afterwards these *q*-orthogonal counterparts were identified as the 3*j* and 6*j* coefficients of the algebra $sl(2,\mathbb{C})q$ [42] (see also [37] for a general review). It is worth recalling that the 3*j* symbol can be obtained, both in the classical and in the *q*-deformed case, as the asymptotic limit of the 6*j* symbol when three of its six entries (not belonging to a same triad) become 'large' in $\hbar$ units. Thus it is not surprising that Racah and *q*-Racah polynomials stand at the top of the so-called Askey and *q*—Askey hierarchies, respectively [17]. Each of the other (*q*-)polynomials of hypergeometric type—depending on either a discrete or continuous variable—(dual Hahn, Jacobi,

V. Aquilanti · A. C. P. Bitencourt · C. da S. Ferreira · M. Ragni (✉)
Dipartimento di Chimica, Università di Perugia,
via Elce di Sotto 8, 06123 Perugia, Italy
e-mail: mirco.ragni@gmail.com

A. Marzuoli
Nazionale di Fisica Nucleare, Sezione di Pavia,
via A. Bassi 6, 27100 Pavia, Italy

Hermite, etc.) fits into the proper hierarchy and can be derived via suitable top-down limiting procedures and/or by specializing previously unconstrained argument(s).

Semiclassical analysis—in particular the study of relationships among families, addition formulas, linearized expressions and various types of sum rules—may look like obscure manipulations of abstract quantities unless a coherent, unifying interpretation arising from physical applications could be disclosed. In the present paper, most mathematical details on hypergeometric hierarchies are necessarily omitted. Rather, an account on Ponzano–Regge asymptotic formula for the 6*j* symbol [63] is given in Sect. 3 as a paradigmatic illustration of the deep interplay between spin network combinatorics and special function theory, on the one hand, and theoretical models underlying the phenomenology of many-body (quantum and semiclassical) systems, on the other.

Such a unifying scenario arising from both the algebraic-combinatorial setting and the analytical asymptotic analysis, as been briefly anticipated in [7]. This developments are resumed in the rest of this paper by resorting to a number of applications, ranging from quantum chemistry and molecular physics (Sect. 4) to quantum computing and discrete quantum gravity models (Sect. 5). An outlook to current and future developments (Sect. 6) concludes the paper.

2 Spin network graphs and combinatorics of *SU*(2) recoupling theory

The basic ingredients needed for the construction of *spin network graphs* are introduced in this section in a quite formalized way, following the treatment presented in the classic book [38] (Topic 12) (see also [55]). At a lower technical level the reader may refer to the book [39] while a more sophisticated approach based on category theory can be found for instance in [49].

Consider $N = (n + 1)$ mutually commuting angular momentum operators of the algebra of $SU(2)$, $\mathbf{J}_1, \mathbf{J}_2, \mathbf{J}_3, \ldots, \mathbf{J}_{n+1} \equiv \{\mathbf{J}_i\}$, and the corresponding components $\{J_{i(z)}\}$ along the quantization axis. For each $i = 1,2,\ldots,n+1$ the simultaneous eigenstates of the complete set $\{\mathbf{J}_i^2, J_{i(z)}\}$ are defined through

$$\mathbf{J}_i^2|j_i m_i\rangle = j_i(j_i+1)\ |j_i m_i\rangle; \quad J_{i(z)}|j_i m_i\rangle = m_i\ |j_i m_i\rangle, \tag{1}$$

where we adopt the convention for which $\hbar = 1$ and the eigenvalues range over

$$j_i = 0, \frac{1}{2}, 1, \frac{3}{2}, \ldots; \quad -j_i \le m_i \le j_i \ \text{(in integer steps)}. \tag{2}$$

Denoting by $\mathcal{H}^{j_i} \doteq \text{span}\{|j_i\, m_i\rangle\}$ the $(2j_i + 1)$-dimensional Hilbert space supporting the j_i-th irreducible representation of $SU(2)$, the tensor product

$$\mathcal{H}^{j_1} \otimes \mathcal{H}^{j_2} \otimes \mathcal{H}^{j_3} \otimes \cdots \otimes \mathcal{H}^{j_n} \otimes \mathcal{H}^{j_{n+1}} \doteq \text{span}\ \{|j_1 m_1\rangle \otimes \cdots \otimes |j_{n+1} m_{n+1}\rangle\} \tag{3}$$

represents the simultaneous eigenspace of the $2(n + 1)$ operators $\{\mathbf{J}_i^2; J_{i(z)}\}$ and may be used *e.g.* to describe the state of $N = (n + 1)$ kinematically independent particles.

To address the interacting case we have to switch to the Wigner-coupled Hilbert spaces of the total angular momentum operator

$$\mathbf{J}_1 + \mathbf{J}_2 + \mathbf{J}_3 + \cdots + \mathbf{J}_{n+1} \doteq \mathbf{J} \tag{4}$$

and of its projection J_z along the quantization axis. The corresponding quantum numbers are J and $M \equiv m_1 + m_2 + \cdots + m_{n+1} (-J \le M \le J \text{in integer steps})$, where the simultaneous eigenspace of the operators $\mathbf{J}^2$ and J_z

$$\mathbf{J}^2|JM\rangle = J(J+1)\ |JM\rangle; \quad J_z|JM\rangle = M\ |JM\rangle \tag{5}$$

turns out to be degenerate. The degeneracy is partially removed by noticing that $\mathbf{J}_1^2, \mathbf{J}_2^2, \ldots, \mathbf{J}_{n+1}^2$ commute with $\mathbf{J}^2$ and J_z and thus j_1, j_2, ...,j_{n+1} are still good quantum numbers (while the individual m_1,m_2,...,m_{n+1} are not). The ket vectors $|JM\rangle$ in Eq. 5 could be rewritten for the moment as $|j_1, j_2, \ldots, j_{n+1}; JM\rangle$, namely in terms of $(n + 1) + 2$ quantum numbers. The complete removal of the degeneracy can be achieved by introducing a new set of $(n - 1)$ Hermitean operators—commuting with each other and with the previous ones—in order to get a total amount of $2(n + 1)$ quantum numbers (this number equals the number of operators needed to specify the eigenstates in the factorized Hilbert space (Eq. 3). The most effective way to reach the goal is to consider binary coupling schemes (binary parenthesization) within the sequence $\mathbf{J}_1 + \mathbf{J}_2 + \mathbf{J}_3 + \cdots + \mathbf{J}_{n+1} = \mathbf{J}$.

As a simple example, consider the case $(n + 1) = 3$: the binary coupling schemes are $(\mathbf{J}_1 + \mathbf{J}_2) + \mathbf{J}_3 = \mathbf{J}$; $\mathbf{J}_1 + (\mathbf{J}_2 + \mathbf{J}_3) = \mathbf{J}$; $(\mathbf{J}_1 + \mathbf{J}_3) + \mathbf{J}_2 = \mathbf{J}$. Then each binary coupling gives rise—by using the Clebsch–Gordan series of $SU(2)$—to an intermediate angular momentum operator whose quantum number will be added to the set $\{j_1, j_2, \ldots, j_{n+1}; JM\}$. In the case $(n + 1) = 3$ the first coupling scheme $(\mathbf{J}_1 + \mathbf{J}_2) + \mathbf{J}_3 = \mathbf{J}$ splits into

$$(\mathbf{J}_1 + \mathbf{J}_2) = \mathbf{J}_{12}; \quad \mathbf{J}_{12} + \mathbf{J}_3 = \mathbf{J} \tag{6}$$

with $|j_1 - j_2| \le j_{12} \le j_1 + j_2$ and $J = j_{12} + j_3$, while the second coupling scheme $\mathbf{J}_1 + (\mathbf{J}_2 + \mathbf{J}_3) = \mathbf{J}$ is specified by

$$(\mathbf{J}_2 + \mathbf{J}_3) = \mathbf{J}_{23}; \quad \mathbf{J}_1 + \mathbf{J}_{23} = \mathbf{J} \tag{7}$$

with $|j_2 - j_3| \le j_{23} \le j_2 + j_3$ and $J = j_1 + j_{23}$.

These alternative 'binary coupled' schemes are graphically represented in terms of 'binary trees with roots', as shown in Fig. 1 (here we agree to associate spin labels to

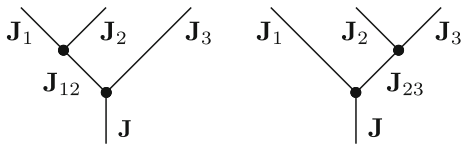

Fig. 1 Alternative, pairwise couplings of three angular momentum operators (which sum up to give a definite total angular momentum) are naturally associated with rooted binary trees. The Hilbert spaces associated with the above binary coupling schemes, although mathematically isomorphic, are not physically equivalent, as far as they correspond to (partially) different complete sets of physical observables, namely $\{\mathbf{J}_1^2, \mathbf{J}_2^2, \mathbf{J}_{12}^2, \mathbf{J}_3^2, \mathbf{J}^2, J_z\}$ and $\{\mathbf{J}_1^2, \mathbf{J}_2^2, \mathbf{J}_3^2, \mathbf{J}_{23}^2, \mathbf{J}^2, J_z\}$, respectively (in particular, $\mathbf{J}_{12}^2$ and $\mathbf{J}_{23}^2$ cannot be measured simultaneously)

the edges of the trees, and not to vertices as done for instance in Appendix A of [55]).

Coming to the general case, a simple counting argument shows that the number of intermediate angular variables arising from a complete binary parenthesization on Eq. 4 is $(n-1)$, plus an external bracket $(...)_J$, thus removing completely the degeneracy in the JM space (Eq. 5). More in details, given a particular binary bracketing structure (keeping fixed for the moment the sequence of incoming angular momenta $\{\mathbf{J}_1, \mathbf{J}_2, \mathbf{J}_3, \ldots, \mathbf{J}_{n+1}\}$), we get a unique set of mutually commuting operators $\mathbf{K}_1, \mathbf{K}_2, \mathbf{K}_3, \ldots, \mathbf{K}_{n-1}$ with quantum numbers $k_1, k_2, k_3, \ldots, k_{n-1}$ respectively, each running over a suitable finite range (*cfr.* what has be done in Eqs. 6 and 7). An explicit example of such a bracketing structure is given by the sequential coupling, represented graphically in Fig. 2. The associated Hilbert space, of dimension $2J+1$, is given by the span of the basis eigenvectors $\{|j_1, j_2, j_3, \ldots, j_{n+1}; k_1, \ldots, k_{n-1}; JM\rangle, -J \leq M \leq J\}$, (here both the sequences of quantum numbers j's and k's are ordered).

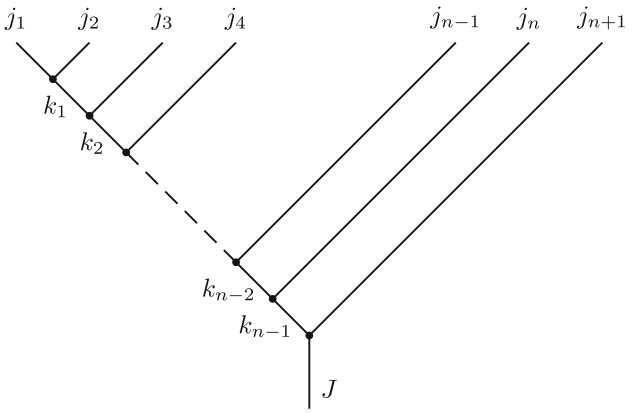

Fig. 2 Sequential binary coupling scheme of $(n+1)$ angular momenta and labelling of intermediate nodes. The associated Hilbert space, of dimension $2J+1$, is given by the span of the basis eigenvectors $\{|j_1, j_2, j_3, \ldots, j_{n+1}; k_1, \ldots, k_{n-1}; JM\rangle, -J \leq M \leq J\}$, (here both the sequences of quantum numbers j's and k's are ordered)

In order to deal with generic binary arrangements of the incoming variables j's and at the same time of the resulting (partially ordered) set of intermediate k's, we adopt notation

$$\{|[j_1, j_2, j_3, \ldots, j_{n+1}]^{\mathfrak{b}}; k_1^{\mathfrak{b}}, k_2^{\mathfrak{b}}, \ldots, k_{n-1}^{\mathfrak{b}}; JM\rangle, \ -J \leq M \leq J\} = \mathcal{H}_n^J(\mathfrak{b}) \doteq \text{span}\ \{\ |\mathfrak{b}; JM\rangle_n\}\ , \tag{8}$$

where the string inside $[j_1, j_2, j_3, \ldots, j_{n+1}]^{\mathfrak{b}}$ is not necessarily ordered, $\mathfrak{b}$ indicates the current binary bracketing structure and the k's are uniquely associated with the chain of pairwise couplings given by $\mathfrak{b}$. The combinatorial structure underlying these binary coupled Hilbert spaces (for fixed n and for any J) is actually provided by the set of all possible *rooted labeled binary trees* (see Appendix A of [55] for more details).[1]

According to the recoupling theory of angular momenta [73, 70] and [38] (Topic 12), the most general *unitary transformation* between two computational states characterized by binary coupling schemes $\mathfrak{b}$ and $\mathfrak{b}'$

$$|[j_1, j_2, j_3, \ldots, j_{n+1}]^{\mathfrak{b}}; k_1^{\mathfrak{b}}, k_2^{\mathfrak{b}}, \ldots, k_{n-1}^{\mathfrak{b}}; JM\rangle \longmapsto |[j_1, j_2, j_3, \ldots, j_{n+1}]^{\mathfrak{b}'}; k_1^{\mathfrak{b}'}, k_2^{\mathfrak{b}'}, \ldots, k_{n-1}^{\mathfrak{b}'}; JM\rangle \tag{10}$$

is implemented by a recoupling coefficient of $SU(2)$ (or $3nj$ symbol) denoted by the shorthand notations

$$\mathcal{U}_{3nj} \begin{bmatrix} k_1^{\mathfrak{b}} & \ldots & k_{n-1}^{\mathfrak{b}} \\ k_1^{\mathfrak{b}'} & \ldots & k_{n-1}^{\mathfrak{b}'} \end{bmatrix} \doteq \mathcal{U}_{3nj}\ [\mathfrak{b}; \mathfrak{b}'], \tag{11}$$

where the variables $\{j\}$, $\{k^{\mathfrak{b}}\}, \{k^{\mathfrak{b}'}\}, J, M$ appearing in states (Eq. 10) have been partially or totally dropped. Then such coefficients represent generalized matrix elements with multiple indices given by the two sets $(k_1^{\mathfrak{b}} \ldots k_{n-1}^{\mathfrak{b}})$ $(k_1^{\mathfrak{b}'} \ldots k_{n-1}^{\mathfrak{b}'})$ and the square modulus $|\mathcal{U}_{3nj}\ [\mathfrak{b}; \mathfrak{b}']|^2$ gives the probability that a quantum system prepared in the state $|\mathfrak{b}; JM\rangle_n$ will be measured in the state $|\mathfrak{b}'; JM\rangle_n$ (note that $\mathcal{U}_{3nj}$ is a 'reduced' tensor operator, namely it does not involve changes in magnetic quantum numbers in view of the Wigner–Eckart theorem).

For each fixed n there exist inequivalent types of $3nj$ symbols: one $6j$ symbol, one $9j$, two $12j$ symbols, five

[1] Recall that any binary coupled basis can be related to the factorized basis (Eq. 3): for instance a vector in the basis associated with the splitting (Eq. 6) can be expanded through

$$|j_1, j_2, j_3; j_{12}; JM\rangle = \sum_{m_1 m_2 m_3} C^{JM}_{j_{12} m_{12} j_3 m_3}\ C^{j_{12} m_{12}}_{j_1 m_1 j_2 m_2}\ |j_1 m_1\rangle \otimes |j_2 m_2\rangle \otimes |j_3 m_3\rangle \tag{9}$$

where there appear two $SU(2)$ Clebsch–Gordan coefficients. This expression can obviously be inverted, providing one factorized basis vector in terms of a combination of binary coupled states in the JM-representation.

15*j*'s, eighteen 18*j*'s etc. [73]. The recoupling coefficients classified as *type I* and *type II* may be expressed through single sums of products of 6*j* symbols, while *types III*, *IV*, *V*,... (appearing for $n \geq 5$) may be represented either by single sums of more complex products of 6*j* and 9*j* symbols or by multiple sums of products of symbols of lower orders. In the present context we do not really need any such expressions since we take advantage of the result proved in [38] (Topic 12) and summarized as follows.

For each n any $\mathcal{U}_{3nj}\,[\mathfrak{b};\mathfrak{b}']$ is the composition of (a finite number of) two elementary unitary transformations, namely

- Racah transform

$$\mathcal{R}\ :|\ldots((ab)_d c)_f \ldots;JM\rangle \mapsto |\ldots(a(bc)_e)_f \ldots;JM\rangle, \qquad (12)$$

- Phase transform

$$\Phi\ :|\ldots(ab)_c \ldots;JM\rangle \mapsto |\ldots(ba)_c \ldots;JM\rangle, \qquad (13)$$

where Latin letters *a*,*b*,*c*,... are used here to denote both incoming (*j*'s in the previous notation) and intermediate (*k*'s) spin quantum numbers.

The explicit expression of Eq. 12 is

$$|(a(bc)_e)_f;M\rangle = \sum_d (-1)^{a+b+c+f}\,[(2d+1)(2e+1)]^{1/2} \times \begin{Bmatrix} a & b & d \\ c & f & e \end{Bmatrix} |((ab)_d c)_f;M\rangle, \qquad (14)$$

where there appears the Racah–Wigner 6*j* symbol of $SU(2)$ and the weights $(2d+1)$, $(2e+1)$ are the dimensions of the irreps labeled by d and e, respectively[2]

Finally, the phase transform (Eq. 13) reads

$$|\ldots(ab)_c \ldots;JM\rangle = (-1)^{a+b-c}\,|\ldots(ba)_c \ldots;JM\rangle. \qquad (15)$$

The above elementary unitary operations satisfy suitable algebraic relations, reflecting the structure of the Racah–Wigner algebra. The Biedenharn–Elliott identity reads

$$\sum_x (-)^{R+x}(2x+1) \begin{Bmatrix} a & b & x \\ c & d & p \end{Bmatrix} \begin{Bmatrix} c & d & x \\ e & f & q \end{Bmatrix} \begin{Bmatrix} e & f & x \\ b & a & r \end{Bmatrix} = \begin{Bmatrix} p & q & r \\ e & a & r \end{Bmatrix} \begin{Bmatrix} p & q & r \\ f & b & c \end{Bmatrix}, \qquad (16)$$

while the Racah identity is expressed as

$$\sum_x (-)^{p+q+x}(2x+1) \begin{Bmatrix} a & b & x \\ c & d & p \end{Bmatrix} \begin{Bmatrix} c & d & x \\ a & b & q \end{Bmatrix} = \begin{Bmatrix} a & c & d \\ b & d & p \end{Bmatrix}, \qquad (17)$$

Here the spin variables $\{a, b, c,\ldots,x\}$ run over $\{0, \frac{1}{2}, 1, \frac{3}{2}, \ldots\}$ and must satisfy suitable triangular inequalities inside each 6*j* symbol (otherwise the symbol itself would vanish). The factor $(2x+1)$ is the dimension of the representation labeled by x, the sum over x is constrained by triangular conditions quoted above, and R in the phase factor of the first identity amounts to $(a+b+c+d+e+f+p+q+r)$.

Note that these identities, together with the orthogonality relation

$$\sum_x (2x+1) \begin{Bmatrix} a & b & x \\ c & d & p \end{Bmatrix} \begin{Bmatrix} c & d & x \\ a & b & q \end{Bmatrix} = \frac{\delta_{pq}}{(2x+1)}, \qquad (18)$$

define uniquely the Racah–Wigner 6*j* symbol, which in turn represents the hypergeometrical polynomial at the top of Askey hierarchy [51] as recalled in the Introduction.

The standard graphical representation of 6*j* (as well as 3*nj*) symbols as Yutsis cubic graphs [73] makes it manifest the combinatorial structure of the objects obtained by joining the edges of two binary trees with the same labels. In particular, referring to the case of three angular momenta of Fig. 1, the associated 6*j* recoupling coefficient is shown in Fig. 3 (where edges are relabeled as $j_1, \ldots, j_6$).

The 9*j* symbol (or Fano X-coefficient) arises naturally when considering two quantum systems described by pure $SU(2)$ angular momentum states endowed with either weak or strong spin-orbit interactions (the corresponding hamiltonians represent two-body conservative interactions and are rotationally invariant operators, namely the magnetic quantum numbers are not active owing to Wigner–Eckart theorem). The two alternative ways of pairing s_1, s_2,l_1,l_2, traditionally referred to as *ls* and *jj* couplings, can be encoded into suitable 'binary trees' whose recoupling

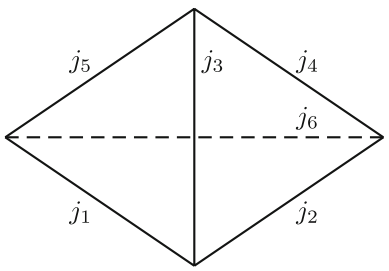

Fig. 3 The 6*j* graphical representation as a complete quadrilateral. The tetrahedral symmetry encoded into the symbol makes it possible to think also of a tetrahedron embedded in Euclidean 3-space with the faces corresponding to the triads in the symbol

[2] In view of the previous footnote, the 6*j* symbol may be expressed as a sum over magnetic quantum numbers of the product of four Clebsch–Gordan coefficients with entries in the set $\{a,b,c,d,e,f; m_a,m_b,m_c,m_d,m_e,m_f\}$, where m_a ($-a \leq m_a \leq a$ in integer steps) is associated with the spin variable a (and similarly for the others), see [70]. The numerical value of the 6*j* symbol depends on normalization: we are tacitly assuming through the whole paper the standard Condon–Shortley conventions.

matrix elements (indeed, the 9*j* coefficient) can be associated with the 3-valent graph depicted in Fig. 4.

With the above examples in mind, it should be clear that binary coupled Hilbert spaces and 3*nj* symbols represent the basic ingredients of a combinatorial construction (leading to general *spin network graphs*) for each fixed integer n ($n \geq 2$). The 'network' structure is denoted by $\mathbf{G}_n(V,E)$, where V and E are the vertex and edge sets of an abstract graph $\mathbf{G}_n$. Both the vertices and the edges (arcs connecting pairs of vertices) of $\mathbf{G}_n(V, E)$ are thus 'decorated' by algebraic objects from $SU(2)$-representation theory introduced above. More precisely, the vertices are in 1–1 correspondence with the set of computational Hilbert spaces $\mathcal{H}_n^J(\mathfrak{b})$ introduced in

$$V \equiv \{v(\mathfrak{b})\} \longleftrightarrow \{\mathcal{H}_n^J(\mathfrak{b})\} \tag{19}$$

while the edge set $E = \{e\}$ of $\mathbf{G}_n(V, E)$ is a subset of the Cartesian product $(V \times V)$ such that an (undirected) arc between two vertices $v(\mathfrak{b})$ and $v(\mathfrak{b}')$

$$e(\mathfrak{b}, \mathfrak{b}') \doteq (v(\mathfrak{b}), v(\mathfrak{b}')) \in (V \times V) \tag{20}$$

exists if, and only if, the underlying Hilbert spaces are related to each other by one of elementary unitary operations defined in Eqs. 12 and 13. The resulting networks are 3-valent (cubic) graphs whose cardinality (number of vertices $|V|$) is given by the so-called quadruple factorial number

$$|V| = \hat{C}_n \equiv \frac{(2n)!}{n!} = (n+1)!C_n, \tag{21}$$

where C_n is the n-th Catalan number. In Fig. 5 the graph $\mathbf{G}_3$ is depicted, where continuous lines correspond to Racah transforms and dashed lines are multiplicative phase factors. Each pentagonal plaquette encodes the Biedenharn–Elliott identity (Eq. 16), while hexagonal plaquettes are associated with Racah identity (Eq. 18) (the oveall phase factor in the latter can be split into three factors, each corresponding to a dashed edge of the plaquette).

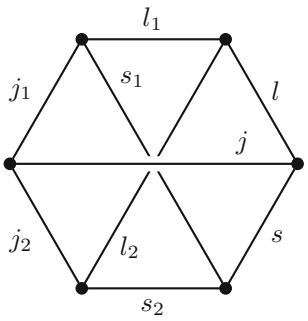

Fig. 4 The Yutsis graph associated with the 9*j* symbol. Labels comply with the classic example of the *ls* and *jj* coupling schemes

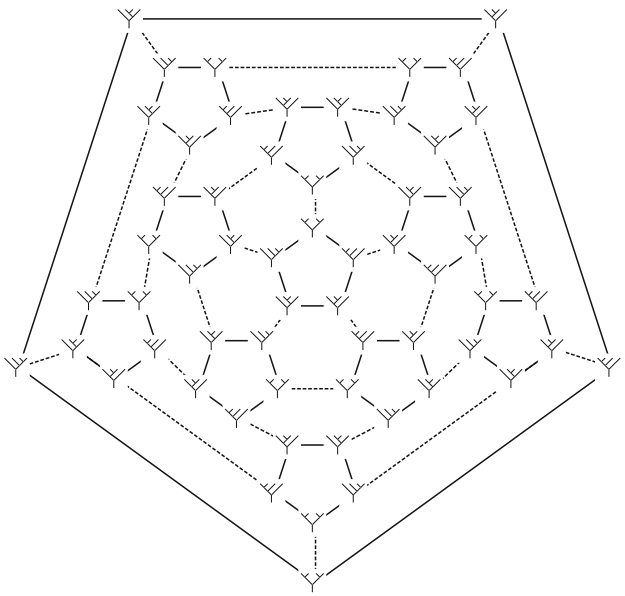

Fig. 5 The spin network graph $\{\mathbf{G}_3$ for $(n+1) = 4$ incoming angular momenta (labels are dropped for simplicity, see [30]). Notice that there appears only one half of the complete graph that would have $\hat{C}_3 = 120$ vertices

3 Asymptotic of spin networks and their semiclassical limits

According to Bohr correspondence principle, classical concepts become increasingly valid in regimes where all (or just a few) quantum numbers are 'large' (as will be discussed in Sect. 4, such regimes are quite commonly encountered in every-day analysis of atomic and molecular dynamical processes).

In handling with angular momenta variables measured in units of $\hbar$, the classical limit $\hbar \to 0$ implies in particular that, for finite angular momenta, the j-quantum numbers and the magnetic ones are much larger than one.

For what concerns in particular pure angular momentum binary coupled states introduced in Eq. 8 of Sect. 2, when approaching classical limit all the components of the vector operators $\{\mathbf{J}_i$ $(i = 1,2,...,n+1)$, $\mathbf{J}\}$ are confined to narrower ranges around specific values. Thus geometrical concepts typical of the semiclassical vector model arise naturally and the corresponding physical quantities have to be thought as averaged out. On the other hand, Racah transform (Eq. 12) admits well defined *asymptotic limits*, whose absolute squares (probabilities) correspond to *classical limits* of the related physical quantities.

Following [63, 67, 68] and [38] (Topic 9) (where a self contained treatment of various asymptotics of angular momentum functions is given, together with the list of original references), consider the case when all the six angular momenta in the 6*j* become large. Recall also that

the square of the symbol has the limiting value given by the Wigner formula

$$\begin{Bmatrix} a & b & d \\ c & f & e \end{Bmatrix} \sim \frac{1}{12\pi V} \tag{22}$$

where V is the Euclidean volume of the tetrahedron formed by the six angular momentum 'vectors' (*cfr*, Fig. 3).

A major breakthrough in semiclassical analysis is provided by the Ponzano–Regge asymptotic formula for the 6*j* symbol [63]

$$\begin{Bmatrix} a & b & d \\ c & f & e \end{Bmatrix} \sim \frac{1}{\sqrt{24\pi V}} \exp\left\{ i\left(\sum_{r=1}^{6} \ell_r \theta_r + \frac{\pi}{4} \right) \right\} \tag{23}$$

where the limit is taken for all entries $\gg 1$ (recall that $\hbar = 1$) and $\ell_r \equiv j_r + 1/2$ with $\{j_r\} = \{a,b,c,d,e,f\}$. V is the Euclidean volume of the tetrahedron with edges of lengths $\{\ell_r\}$, calculated by using the Cayley determinant (note the shift $j \to j + 1/2$ with respect to the variables employed in calculating the volume in Eq. 22 and finally θ_r is the angle between the outer normals to the faces which share the edge ℓ_r.

The probability amplitude (Eq. 23) has the form of a semiclassical wave function since the factor $1/\sqrt{24\pi V}$ is slowly varying with respect to the spin variables, while the exponential is a rapidly oscillating dynamical phase (such behavior complies with Wigner's formula (Eq. 22). Moreover, according to Feynman path sum interpretation of quantum mechanics, the argument of the exponential represents a classical action, and indeed it can be read as $\sum p\dot{q}$ for pairs (p,q) of canonical variables (angular momenta and conjugate angles). A sophisticated analysis of asymptotic limits of coupling and recoupling coefficients based on the theory of quantum and semiclassical integrable systems can be found in [33].

Another interesting issue—arising in connection with the interpretation of spin networks as computational quantum graphs—concerns the phenomenon of *disentaglement*. According to definitions given in Sect. 2, one of the main features of states belonging to the binary coupled Hilbert spaces (Eq. 8) is to represent effectively 'entangled' quantum states (namely states that cannot be reduced to a product of states containing quantum numbers of the individual components as in Eq. 3. Recall also that the 6*j* symbol (Eq. 12), being a transition amplitude, takes care of the fact that the operators $\mathbf{J}_d^2$ and $\mathbf{J}_e^2$ (with quantum numbers d and e respectively) do not belong to the same set of mutually commuting operators and thus cannot be measured simultaneously. However, in the semiclassical limit given in Eq. 23 the six entries of the 6*j* symbol appear on the same footing, a feature that can be interpreted as a 'disentanglement' of the underlying 'semiclassical' spin networks.

In [5] the first nontrivially entangled network given by the 9*j* symbol (Fig. 4) is addressed. The basics of asymptotic approximations when some of the entries are large are presented and numerical calculations which illustrate the passage to the semiclassical limit are carried out. The semiclassical analysis of such a symbol is more complicated with respect to Ponzano–Regge case (Eq. 23), but nevertheless the general features described above, namely the occurrence of disentangling and the discrete–continuum transition, are made manifest. The analytical and numerical study of semiclassical expansions of 3*nj* symbols for $n > 2$, as well as of different types of asymptotics (in which only a few variables are large, while the other ones are kept 'quantized'), represents a major challenge not only in the framework of the formal theory of hypergeometric polynomials and related hierarchies [51], but also in view of applications to specific physical problems, to be discussed next.

4 Molecular Physics and quantum chemistry

4.1 Molecular spectroscopy and atomic collisions: Hund's cases

A presentation of angular momentum theory from the viewpoint of these applications, is given by Zare [74]. The theory developed about thirty years ago in [31] dealt with five alternative representations for the quantum-mechanical close-coupling formulation [14, 31, 32] of the motion along the internuclear distance of a vibrating diatomic molecule or colliding atoms having internal (spin and/or electronic) angular momenta. This unified frame transformation approaches of atomic collision theory and concepts of molecular spectroscopy, is originally due to Hund. The physical picture and the relevant nomenclature are reviewed in [27], see also [28]. Explicitly [24], starting from a sum rule equivalent to the Biedenharn–Elliott relation (a pentagonal closed path on the abacus of Fig. 5, see also [30] and [7]), we obtain the definition of a 6*j* symbol as a sum of four 3*j* symbols by taking a proper limit, since one angular momentum is much larger than the others [27]. The coupling schemes of four angular momenta are illustrated in [27] as the basic ingredients underlying the classification of the five Hund cases and the relationships among representations. It was shown that the transition from one coupling scheme to another is performed by an orthogonal transformation whose matrix elements can be written in terms of 6*j* symbols. In the pentagonal arrangement of five alternative coupling schemes for four angular momenta (represented by the tree-like graphs at the vertices) [24], connections (the sides

of the pentagon) are realized by orthogonal matrices and are related to 6*j* symbols. This was the archetype for the abacus in Fig. 5, see also Fig. 1 of [7] and [30]. Recent extensions of this approach has shown that in a general theory of interacting open shell atoms, 3*nj* symbols up to $n = 6$ occur [52].

4.2 Hyperquantization algorithm

An important message that we have learned from work reviewed in Sect. 1 is the view that a continuous variable limit is obtained at high angular momenta from the discrete structure typical of quantum mechanics. The opposite viewpoint can be considered as well, namely the semiclassical limit may describe a continuous structure, and quantum angular momentum algebra provides discretization.

The search for both alternative reference frames and angular momentum coupling schemes has been a major challenge in quantum mechanics since its origin, and tranformations among them are represented by vector–coupling and recoupling coefficients, respectively. The relevant equations can then be formulated in terms of quantum numbers, which approximately correspond to constants of motion of the systems under study. Fundamental advances have been achieved over the years within this framework: in the last Fifties Jacob and Wick introduced the helicity formalism, widely used for the theoretical treatment of a variety of collisional problems; extending Hund's introduction of alternative coupling schemes for a diatomic molecule carrying electronic, spin, and rotational angular momenta (See Sect. 1). These developments fit into the frame transformation theory pioneered by Fano and coworkers in the Seventies.

Indeed, for general anisotropic interaction, discretization procedures can be introduced by exploiting Racah algebra, which fosters the introduction of alternative coupling schemes labeled by 'artificial' quantum numbers. This method has been shown to provide an elegant and powerful tool for the solution of the reactive scattering Schröndinger equation and, at present, a considerable number of methods have been developed in this spirit, among which the 'hyperquantization' algorithm, outlined in greater detail in a number of references [22, 24, 29]. The technique relies on the hyperspherical coordinate approach when used for few-body processes, including rearrangement. For instance, in a reactive triatomic process, the reaction coordinate is represented by the hyperradius, which is a measure of the total inertia of the system, and an adiabatic representation of the total eigenfunction with respect to this coordinate is adopted. In such a way, a quantization problem on the surface of the a hypersphere (in this case the sphere in a 6-dimensional Euclidean space) must be solved for fixed values of the hyperradius. Then coupled-channel equations are integrated applying a standard propagation procedure. The success of this approach is strictly dependent on the accuracy and the effectiveness of the method used to solve the fixed hyperradius problem. The computation of the adiabatic eigenvalues containing detailed information on the structure, rotations, and internal modes parametrically in the hyperrradius is typically very demanding. The hyperquantization algorithm exploits the peculiar properties of the discrete analogues of hyperspherical harmonics, i.e., generalized 3*j* symbols or Hahn polynomials, orthogonal on a grid of points that span the interaction region [21]. The computationally advantageous aspect of this algorithm, besides the elegance of unifying under the language of angular momentum theory the dynamical treatment of a reaction, is the structure of the Hamiltonian matrix: its kinetic part is simple, universal, highly symmetric, and sparse, while the potential displays the diagonal form characteristic of the stereodirected representations of the previous section. The hyperquantization algorithm, when implemented for reactive scattering calculations [24], allows considerable savings in memory requirements for storage and in computing time for the building up and diagonalization of large basis sets, exploiting the sparseness and the symmetry properties of the Hamiltonian matrix.

4.3 Reaction dynamics and quantum chemistry

Reference of these techniques iv aspects of reaction theory [19] and of quantum chemistry [15, 16, 18, 20].

In Sect. 2, we have outlined how the concepts of reference frame transformations and of alternative angular momentum coupling schemes in quantum mechanics lead to different representations of the quantum scattering matrix and provide a powerful guide for the analysis of atomic and molecular collisions. In particular, we have exemplified atomic and molecular elastic and inelastic collisions, but extensions to reactive scattering are most interesting and extensive applications have been worked out. Dynamical calculations for the system $He + H_2^+$ [13, 62] and for the benchmark reaction $F + H_2$[25, 23] have been performed, also including fine-structure and isotopic effects on reactivity.

Also, a new class of entrance and exit channel indices in the scattering matrix has been worked out. Through the hyperspherical coordinate formulation referred to in Sect. 2, the hyperrradial problem is essentially equivalent to that of scattering from anisotropic potentials, and such a "stereodirected representation" of the scattering matrix can be used to derive information about the stereodynamincs of an atom–diatom reaction. A quantity that can be reconducted to properties measured in beam experiments on oriented

molecules is the reaction probabilitiy as a function of the *steric quantum number* (see *e.g.* [28]).

Since present quantum-mechanical calculations are becoming feasible for reactive encounters on realistic potential energy surfaces (the hyperquatization algorithm provides an efficient machinery in this direction), stereodynamical properties exploiting the stereodirected representation have been reported, specifically for the reaction of HF with Li [2, 3] and of F with H_2 [1].

Further perspectives concerning the extension of angular momentum theory to hyperspaces and the use of modern advances in the theory of orthogonal polynomials of a discrete variable have been reviewed [11]. Among applications, it is worth mentioning the possibility of representing polarization parameters by 'discrete' multipole moments [4, 6] and potential energy surfaces by orthogonal discrete basis sets [12].

The study of asymptotic expansions of $3nj$ symbols for $n > 2$, as well as of different types of asymptotics (in which only a few variables are large, while the other ones are kept 'quantized') represents a major challenge not only in the framework of the formal theory of hypergeometric polynomials and related hierarchies [51], but also in view of applications to specific physical problems arising in connections with all the topics discussed in the previous Sect. 4 and 5. A key example is the crucial occurrence of $9j$ symbols in the many center problem in quantum chemistry, either in Sturmian orbital or in momentum space approaches [8, 36].

5 Quantum gravity and quantum computing

5.1 Discretized quantum gravity

There exists an intriguing physical interpretation of the Ponzano–Regge asymptotics (Eq. 23) once we recognize that the expression in the exponential represents the classical Regge action [64]—namely the discretized version of Einstein–Hilbert action of General Relativity—for the tetrahedron associated with the $6j$ symbol in the semiclassical limit. In Fig. 3 the tetrahedral symmetry of the $6j$ symbol was made manifest by associating its six entries with edges and its four triads with faces of a tetrahedron embedded in Euclidean 3-space.

In Regge's approach to General Relativity, the edge lengths of a 'triangulated spacetime' are taken as discrete counterparts of the metric tensor appearing in the usual action for gravity and angular variables (deficit angles) are related to the scalar curvature obtained from the Riemann tensor. Technically speaking, a Regge spacetime is a piecewise linear (PL) manifold of dimension D dissected into simplices, namely triangles in $D = 2$, tetrahedra in $D = 3$, 4-simplices in $D = 4$ and so on. Inside each simplex either an Euclidean or a Minkowskian metric can be assigned: accordingly, spacetime manifolds obtained by gluing together D-dimensional simplices acquire an overall *PL* metric of Riemannian or Lorentzian signature.

'Regge Calculus' became in the early 1980s the starting point for a novel approach to quantization of General Relativity known as simplicial quantum gravity (see the reviews [65, 72] and references therein). The quantization procedure most commonly adopted is the Euclidean path sum approach, namely the discretized version Feynman path integral describing D-dimensional geometries undergoing 'quantum fluctuations'. According to this prescription, the asymptotic functional (Eq. 23)—to be understood here as the semiclassical limit of a sum over truly 'quantum' fluctuations—turns out to be associated with the simplest 3-dimensional 'spacetime', the Euclidean tetrahedron. The construction of the so-called Ponzano–Regge 'state sum' representing the quantum partition function of simplicial 3-gravity can be sketched as follows.

Denote by $\mathcal{T}^3(j) \to \mathcal{M}^3$ a particular triangulation of a closed 3-dimensional PL manifold $\mathcal{M}^3$ (of fixed topology) obtained by assigning $SU(2)$ 'spin variables' $\{j\}$ to the edges of $\mathcal{T}^3$. The assignment must satisfy a number of conditions which can be more easily illustrated if we introduce the state functional associated with $\mathcal{T}^3(j)$, namely

$$\mathbf{Z}[\mathcal{T}^3(j) \to \mathcal{M}^3; L] = \Lambda(L)^{-N_0} \prod_{A=1}^{N_1} (-1)^{2j_A} \mathtt{w}_A \prod_{B=1}^{N_3} \phi_B \left\{ \begin{matrix} j_1 & j_2 & j_3 \\ j_4 & j_5 & j_6 \end{matrix} \right\}_B$$

where N_0, N_1, N_3 denote the number of vertices, edges and tetrahedra in $\mathcal{T}^3(j)$, $\Lambda(L) = 4L^3/3C$ (C an arbitrary constant), $\mathtt{w}_A \doteq (2j_A + 1)$ is the dimension of the irreducible representation j_A of $SU(2)$ placed on the A-th edge, $\phi_B = (-1)^{\sum_{p=1}^{6} j_p}$ and $\{:::\}$'s are $SU(2)$ $6j$ symbols to be associated with the tetrahedra of the triangulation. The Ponzano–Regge state sum is obtained by summing over triangulations corresponding to all assignments of spin variables $\{j\}$ bounded by the cut-off L, namely

$$\mathbf{Z}_{PR}[\mathcal{M}^3] = \lim_{L \to \infty} \sum_{\{j\} \leq L} \mathbf{Z}\,[\mathcal{T}^3(j) \to \mathcal{M}^3; L] \tag{25}$$

where the cut-off is formally removed by taking the limit in front of the sum. As already noted in [63] (see also [38] (Topic 9)), the above state sum is a topological invariant since its value is independent of the particular triangulation, namely does not change under suitable combinatorial transformations. Quite interestingly, such 'topological moves' are actually encoded algebraically into the Biedenharn–Elliott identity (Eq. 16) and the orthogonality condition (Eq. 18), see e.g., [55] (Sect. 5) for more details.

Several years after Ponzano–Regge paper, a regularized version of Eqs. 24 and 25, based on representation theory of a

quantum deformation of the group $SU(2)$ at $q = \exp\{2\pi i/k\}, k \geq 2$ integer—was proposed in [69] and shown to be a well-defined (finite) topological invariant for closed 3-manifolds. Since then there has been a renewed interest also in the asymptotics (Eq. 23) both in connection with the study of 3-manifold geometry [61] (and higher-dimensional generalizations [40]) and in addressing 'loop quantum gravity' models, see [66, 43] and references therein.

5.2 Quantum automata and topological invariants

In the past few years, there has been a tumultuous activity aimed at introducing novel conceptual schemes for quantum computing. The model of quantum simulator proposed in [54, 55] and further discussed in [56, 57] relies on the recoupling theory of $SU(2)$ angular momenta discussed in Sect. 2 and can be viewed as a generalization to arbitrary values of the spin variables of the usual quantum-circuit model based on 'qubits' and Boolean gates [59]. The basic ingredient of such general scheme for universal quantum computing are indeed encoded into spin network computational graphs of the type depicted in Fig. 5. Such pictorial representation makes it clear that the computational space of the simulator complies with the architecture of (families of) 'automata'. An automaton in computer science is a graph whose nodes encode 'internal states' while a link between two nodes represents an admissibile operation or 'transition' between the corresponding states (*cfr*. [58, 71] for an account on quantum automaton models). According with this kind of interpretation, a computational process on the spin network can be associated with a directed path, namely an ordered sequence of vertices and edges starting from an initial quantum state, say $|s>_{\text{in}}$, and ending in some set of final states $\{|s>_{\text{fin}}\}$.

In a series of papers [44–48] families of automata arising from the q-deformed analog of the spin network simulator have been implemented in order to deal with classes of computationally-hard problems in geometric topology (topological invariants associated with knots and with closed 3-dimensional manifolds).[3]

From the point of view of classical complexity theory, computing such invariants is 'hard', namely could be achieved by a classical computer only by resorting to an exponential amount of resources. A computational process which requires an amount of resources that grows at most polynomially with the size of the computational problem is referred to as 'efficient' (*cfr*. In [46] and references therein for an account of algorithmic questions involving braid group and topological invariants of knots).

In [45, 47], efficient (i.e., running in polynomial time) quantum algorithms for approximating, within an arbitrarily small range, $SU(2)_q$-colored polynomial invariants of knots have been explicitly worked out. More precisely, this algorithmic problem has been recognized to be 'complete' in the computational class **BQP** (Bounded error Quantum Polynomial). This means that each algorithmic problem in this class can be efficiently reduced to an evaluation of such a topological invariant for a proper knot. In [44] such algorithms have been generalized to deal with 3-manifold invariants, while in [48] connections among quantized geometries (Sect. 1), topological quantum field theory and quantum computing are discussed in detail.

6 Outlook

The paper [33] deals with a systematic study of the asymptotics of the $3j$ Wigner symbol from the standpoint of semiclassical mechanics, that is, essentially multimensional WKB theory for integrable systems. Such asymptotics represents a matrix element connecting eigenfunctions of a pair of integrable systems, obtained by lifting the problem of the addition of angular momenta into the space of Schwinger's oscillators. A novel element is the appearance of compact Lagrangian manifolds that are not tori, due to the fact that the observables defining the quantum states are not commuting. These manifolds can be quantized by generalized Bohr–Sommerfeld rules and yield all the correct quantum numbers. Such an approach makes it manifest the geometry of the classical angular momentum vectors and allows efficient methods for computing amplitude determinants in terms of Poisson bracket. Extension of such geometrical methods to the cases of $6j$ and $9j$ symbols are currently under study.

An interesting issue related to the previous remarks—as well as to algorithmic problems addressed in Sect. 2—is about 'efficient computability' of $3nj$ symbols. These 'Yutsis' cubic graphs are listed explicitly up to $n = 6$, and for a fixed n there are different numbers of non-isomorphic configurations, each corresponding to an inequivalent quantum transition amplitude given by the square modulus of the associated $3nj$ [73]. Open questions are: to decide whether a trivalent graph is a Yutsis graph; to find the most efficient way of splitting $3nj$ symbols into sums of products of $6j$ symbols; to understand the origin of the sequence: 1, 1, 2, 5, 18, (...) given by Yutsis for the numbers of inequivalent $6j$, $9j$, $12j$, $15j$, $18j$, (...) symbols, just to mention a few. In particular, the theoretical computational complexity encoded into recurrence relations [70] involving the coefficients should be addressed at least for the simplest cases (see [5] for a preliminary numerical analysis of the $9j$).

[3] A topological invariant is a quantity—typically a number or a polynomial—that depends only on the global topology of the geometrical object and not on its local metric properties, see [61] for definitions and original references.

Besides q-deformed counterparts, alternative extensions of 'spin networks' are studied in [26], where 'ternary trees' are introduced to represent graphically the basic features of 'elliptic' coordinate sets on S^2 and S^3 [S^d denotes the standard d-sphere embedded in the $(d+1)$-dimensional Euclidean space] and of the corresponding harmonics. Interestingly, continuously moving along the edges of the abacus of Fig. 5 can be associated to the variation of the modulus of elliptic functions [9, 10, 34]. In [41] symmetric couplings of three angular momenta—instead of binary couplings as depicted in Fig. 1—are associated with eigenstates of a 'volume operator', and transition amplitudes between the latter and the standard binary ones are worked out in the semiclassical limits. All these kinds of extensions to non-standard coupling and recoupling schemes and their asymptotic expansions deserve further investigation in order to characterize the action functionals of the underlying physical systems.

Finally, for what concerns the issues discussed in Sect. 5, further algorithmic problems regarding (spin network-type) quantum geometry, topological quantum field theories in dimension 3 and associated 2-dimensional lattice models (as well as relations among them) are currently under study [50].

The issues discussed in this paper make it manifest that $SU(2)$ recoupling theory provides not only powerful algebraic, combinatorial and analytical techniques for addressing concrete problems in several different fields, but does represent a unifying framework. This perspective can be further stretched to cover the theory of formal languages and associated families of abstract (quantum) computing machines [53].

Acknowledgments This work has been partially supported by Italian MIUR and ASI Agencies. The authors would like to thank Roger Anderson, Mauro Carfora, Robert Littlejohn and Mario Rasetti for interesting discussions. Doctoral fellowships to ACPB by Capes, Brazil, and to CSF by Alban, EU, are also gratefully acknowledged.

References

1. Aldegunde J, Alvariño JM, De Fazio D, Cavalli S, Grossi G, Aquilanti V (2004) Quantum stereodynamics of the F + H_2 → HF + H reaction by the stereodirected s-matrix approach. Chem Phys 304:251–259
2. Alvariño JM, Aquilanti V, Cavalli S, Crocchianti S, Laganà A, Martinez T (1997) Exact quantum stereodynamics: the steric effect for the Li + HF → LiF + H reaction. J Chem Phys 107:3339–3340
3. Alvariño JM, Aquilanti V, Cavalli S, Crocchianti S, Laganà A, Martinez T (1998) Stereodynamics from the stereodirected representation of the exact quantum S matrix :the Li + HF → LiF + H reaction. J Phys Chem A 102:9638–9644
4. Anderson RW, Aquilanti V (2006) The discrete representation correspondence between quantum and classical spatial distributions of angular momentum vectors. J Chem Phys 124:214,104 (9 pages)
5. Anderson RW, Aquilanti V, da Silva Ferreira C (2008) Exact computation and large angular momentum asymptotics of 3nj symbols: semiclassical disentangling of spin networks. J Chem Phys 129:161,101–161,105
6. Aquilanti V, Ascenzi D, Cappelletti D, Fedeli R, Pirani F (1997) Molecular beam scattering of nitrogen molecules in supersonic seeded beams: a probe of rotational alignment. J Phys Chem A 101:7648–7656
7. Aquilanti V, Bitencourt ACP, da Silva Ferreira C, Marzuoli A, Ragni M (2008) Quantum and semiclassical spin networks: from atomic and molecular physics to quantum computing and gravity. Phys Scr 78:058–103
8. Aquilanti V, Caligiana A (2002) Sturmian approach to one-electron many-center systems: integrals and iteration schemes. Chem Phys Lett 366:157–164
9. Aquilanti V, Caligiana A, Cavalli S (2003) Hydrogenic elliptic orbitals, coulomb sturmian sets. Recoupling coefficients among alternative bases. Int J Quant Chem 92:99–117
10. Aquilanti V, Caligiana A, Cavalli S, Coletti C (2003) Hydrogenic orbitals in momentum space and hyperspherical harmonics. Elliptic sturmian basis sets. Int J Quant Chem 92:212–228
11. Aquilanti V, Capecchi G (2000) Harmonic analysis and discrete polynomials. from semiclassical angular momentum theory to the hyperquantization algorithm. Theor Chem Accounts 104:183–188
12. Aquilanti V, Capecchi G, Cavalli S, Adamo C, Barone V (2000) Representation of potential energy surfaces by discrete polynomials: proton transfer in malonaldehyde. Phys Chem Chem Phys 2:4095–4103
13. Aquilanti V, Capecchi G, Cavalli S, De Fazio D, Palmieri P, Puzzarini C, Aguilar A, Giménez X, Lucas JM (2000) The HE + H_2^+ reaction: a dynamical test on potential energy surfaces for a system exhibiting a pronounced resonance pattern. Chem Phys Lett 318:619–628
14. Aquilanti V, Casavecchia P, Laganà A, Grossi G (1980) Decoupling approximations in the quantum mechanical treatment of p-state atom collisions. J Chem Phys 73:1173–1180
15. Aquilanti V, Cavalli S, Coletti C (1997) The d-dimensional hydrogen atom: hyperspherical harmonics as momentum space orbitals and alternative sturmian basis sets. Chem Phys 214:1–13
16. Aquilanti V, Cavalli S, Coletti C (1998) Hyperspherical symmetry of hydrogenic orbitals and recoupling coefficients among alternative bases. Phys Rev Lett 80:3209–3212
17. Aquilanti V, Cavalli S, Coletti C (2001) Angular and hyperangular momentum recoupling, harmonic superposition and racah polynomials. a recursive algorithm. Chem Phys Lett 344:587–600
18. Aquilanti V, Cavalli S, Coletti C, Di Domenico D, Grossi G (2001) Hyperspherical harmonics as sturmian orbitals in momentum space: a systematic approach to the few-body coulomb problem. Int Rev Phys Chem 20:673–709
19. Aquilanti V, Cavalli S, Coletti C, De Fazio D, Grossi G (1996) Hyperangular momentum: Applications to atomic and molecular science. In: Tsipis CA, Popov VS, Herschbach DR, Avery JS (eds) New Methods in Quantum Theory. Kluwer, Dordrecht pp 233–250
20. Aquilanti V, Cavalli S, Coletti C, Grossi G (1996) Alternative sturmian bases and momentum space orbitals: an application to the hydrogen molecular ion. Chem Phys 20:405–419
21. Aquilanti V, Cavalli S, De Fazio D (1995) Angular and hyperangular momentum coupling coefficients as Hahn polynomials. J Phys Chem 99:15,694–15,698
22. Aquilanti V, Cavalli S, De Fazio D (1998) Hyperquantization algorithm: I. theory for triatomic systems. J Chem Phys 109:3792–3804
23. Aquilanti V, Cavalli S, De Fazio D, Volpi A, Aguilar A, Giménez X, Lucas J (2002) Exact reaction dynamics by the hyperquantization algorithm: integral and differential cross section for F + H_2, including long-range and spin-orbit effects. Phys Chem Chem Phys 4:401–415

24. Aquilanti V, Cavalli S, De Fazio D, Volpi A, Aguilar A, Giménez X, Lucas JM (1998) Hyperquantization algorithm: II. implementation for the F + H_2 reaction dynamics including open-shell and spin-orbit interaction. J Chem Phys 109:3805–3818
25. Aquilanti V, Cavalli S, De Fazio D, Volpi A, Aguilar A, Giménez X, Lucas JM (1999) Probabilities for the F + H_2 → HF + H reaction by the hyperquantization algorithm: alternative sequential diagonaliation schemes. Phys Chem Chem Phys 1:1091–1098
26. Aquilanti V, Cavalli S, Grossi G (1986) Hyperspherical coordinates for molecular dynamics by the method of trees and the mapping of potential energy surfaces for triatomic systems. J Chem Phys 86:1362–1375
27. Aquilanti V, Cavalli S, Grossi G (1996) Hund's cases for rotating diatomic molecules and for atomic collisions: angular momentum coupling schemes and orbital alignment. Z Phys D 36:215–219
28. Aquilanti V, Cavalli S, Volpi A (2000) Angular momentum coupling schemes for molecular collisions: the stereodirected representation. Phys Essays 13:412–420
29. Aquilanti V, Cavalli S, Volpi A, De Fazio D (2001) The a+bc reaction by the hyperquantization algorithm: the symmetric hyperspherical parametrization for $j > 0$. Adv Quant Chem 39:103–121
30. Aquilanti V, Coletti C (2001) 3nj-symbols and harmonic superposition coefficients: an icosahedral abacus. Chem Phys Lett 344:601–611
31. Aquilanti V, Grossi G (1980) Angular momentum coupling schemes in the quantum mechanical treatment of p-state atom collisions. J Chem Phys 73:1165–1172
32. Aquilanti V, Grossi G, Laganà A (1981) Approximate selection rules for intramultiplet and depolarization cross sections in atomic collisions. Nuovo Cimento B 63:7–14
33. Aquilanti V, Haggard HM, Littlejohn R, Yu L (2007) Semiclassical analysis of Wigner 3*j*-symbol. J Phys A 40:5637–5674
34. Aquilanti V, Tonzani S (2004) Three-body problem in quantum mechanics: hyperspherical elliptic coordinates and harmonic basis sets. J Chem Phys 120(9):4066–4073
35. Askey R, Wilson J (1979) A set of orthogonal polynomials that generalize the Racah coefficients or 6−*j* symbols. SIAM J Math Anal 10:1008
36. Avery J, Avery J (2006) Generalized sturmians and atomic spectra. World Scientific, Singapore
37. Biedenharn LC, Lohe MA (1995) Quantum group symmetry and q-tensor algebras. World Scientific, Singapore
38. Biedenharn LC, Louck JD (1981) The Racah–Wigner algebra in quantum theory. In: Rota GC (ed) Encyclopedia of mathematics and its applications, vol 9. Addison-Wesley, Reading
39. Brink DM, Satchler GR (1998) Angular momentum, 2nd edn. Oxford Library of The Physical Sciences, New York
40. Carbone G, Carfora M, Marzuoli A (2001) Hierarchies of invariant spin models. Nucl Phys B 595:654–688
41. Carbone G, Carfora M, Marzuoli A (2002) Quantum states of elementary 3-geometry. Class Quantum Grav 19:3761–3774
42. Faddeev L, Reshetikhin N, Takhtajan L (1990) Quantum Lie groups and Lie algebras. Leningrad Math 1:193–225
43. Freidel L, Krasnov K. A new spin foam model for 4d gravity. arXiv:0708.1595 [gr-qc]
44. Garnerone S, Marzuoli A, Rasetti M. Efficient quantum processing of 3-manifold topological invariants. arXiv: quant-ph/0703037
45. Garnerone S, Marzuoli A, Rasetti M (2006) Quantum computation of universal link invariants. Open Sys Infor Dyn 13:373–382
46. Garnerone S, Marzuoli A, Rasetti M (2006) Quantum knitting. Laser Phys 11:1582–1594
47. Garnerone S, Marzuoli A, Rasetti M (2007) Quantum automata, braid group and link polynomials. Quant Inform Comp 7:479–503
48. Garnerone S, Marzuoli A, Rasetti M (2007) Quantum geometry and quantum algorithms. J Phys A Math Theor 40:3047–3066
49. Joyce WP (2001) Diagram projection rules for recoupling diagrams in the Racah–Wigner category. J Math Phys 42:1346–1363
50. Kàdàr Z, Marzuoli A, Rasetti M (2008) Braiding and entanglement in spin networks: a combinatorial description of topological phases. Int J Quantum Inf (in press). arXiv:0806.3883
51. Koekoek R, Swarttouw R (1998) The Askey-scheme of hypergeometric orthogonal polynomials and its q-analogue. Technical report, TU Delft, The Netherlands. Anonymous ftpsite: ftp://twi.tudelft.nl, directory:/pub/publications/tech-reports
52. Krems RV, Groenenboom GC, Dalgarno A (2004) Electronic interaction anisotropy between atoms in arbitrary angular momentum states. J Phys Chem A 108:8941–8948
53. Marzuoli A, Rasetti M (in preparation)
54. Marzuoli A, Rasetti M (2002) Spin network quantum simulator. Phys Lett A 306:79–87
55. Marzuoli A, Rasetti M (2005) Computing spin networks. Ann Phys 318:345–407
56. Marzuoli A, Rasetti M (2005) Spin network setting of topological quantum computation. Int J Quant Inf 3:65–72
57. Marzuoli A, Rasetti M (2007) Coupling of angular momenta: an insight into analogic/discrete and local/global models of computation. Nat Computing 6:151–168
58. Moore C, Crutchfield JP. Quantum automata and quantum grammars. arXiv: quant-ph/ 9707031
59. Nielsen MA, Chuang IL (2008) Quantum computation and quantum information. Cambridge University Press, Cambridge
60. Nikiforov AF, Suslov SK, Uvarov VB (1991) Classical orthogonal polynomials of a discrete variable. Springer, Berlin
61. Ohtsuki T (2002) Problems on invariants of knots and 3-manifolds, rims geometry and topology monographs. eprint math. GT/0406190 4:377–572
62. Palmieri P, Puzzarini C, Aquilanti V, Capecchi G, Cavalli S, De Fazio D, Aguilar A, Giménez X, Lucas JM (2000) Ab initio dynamics of the He + H_2^+ → HeH^+ + H reaction: a new potential energy surfaces and quantum mechanical cross sections. Mol Phys 98:1835–1849
63. Ponzano G, Regge T (1968) Semiclassical Limit of Racah coefficients. In: Bloch F et al (eds) Spectroscopic and group theoretical methods in physics. North-Holland, Amsterdam
64. Regge T (1961) General relativity without coordinates. Nuovo Cimento 19:558–571
65. Regge T, Williams RM (2008) Discrete structures in gravity. J Math Phys 41:3964–3984
66. Rovelli C (2007) Quantum gravity. Cambridge University Press, Cambridge
67. Schulten K, Gordon RG (1975) Exact recursive evaluation of 3*j*- and 6*j*-coefficients for quantum-mechanical coupling of angular momenta. J Math Phys 16:1961–1970
68. Schulten K, Gordon RG (1975) Semiclassical approximations to 3*j* and 6*j*-coefficients for quantum-mechanical coupling of angular momenta. J Math Phys 16:1971–1988
69. Turaev V, Viro OY (1992) State sum invariants of 3-manifolds and quantum-6*j* symbols. Topology 31:865–902
70. Varshalovich DA, Moskalev AN, Khersonskii VK (1988) Quantum theory of angular momentum. World Scientific, Singapore
71. Wiesner K, Crutchfield JP. Computation in finitary stochastic and quantum processes. arXiv: quant-ph/ 0608206
72. Williams RM (1992) Regge calculus: a bibliography and brief review. Class Quantum Grav 9:1409–1422
73. Yutsis AP, Levinson IB, Vanagas VV (1962) Mathematical apparatus of the theory of angular momentum. Israel Program for Scientific Translation, Jerusalem
74. Zare RN (1988) Angular momentum. Wiley, London